

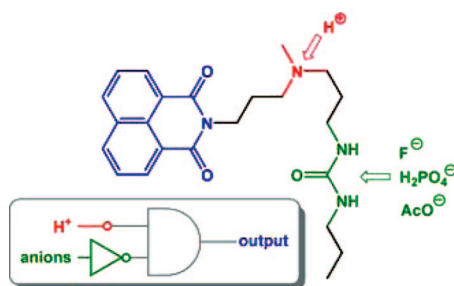
## Modular Functional Integration of a Two-Input INH Logic Gate with a Fluorophore–Spacer–Receptor<sub>1</sub>–Spacer–Receptor<sub>2</sub> Conjugate

Marek Kluciar,<sup>†,‡</sup> Rita Ferreira,<sup>§</sup> Baltazar de Castro,<sup>†</sup> and Uwe Pischel<sup>\*,§</sup>

Department of Chemical Engineering, Physical Chemistry, and Organic Chemistry, Faculty of Experimental Sciences, University of Huelva, Campus de El Carmen s/n, E-21071 Huelva, Spain, and REQUIMTE/Department of Chemistry, Faculty of Sciences, University of Porto, Rua Campo Alegre, 4169-007 Porto, Portugal

uwe.pischel@diq.uhu.es

Received February 10, 2008



The synthesis and photophysical characterization of a fluorophore–spacer–receptor<sub>1</sub>–spacer–receptor<sub>2</sub> system, which combines the 1,8-naphthalimide fluorophore with amine and urea receptor units, is reported. Photoinduced electron transfer (PET) from the amino group was blocked by protonation, leading to a drastic fluorescence enhancement (ca. 20 times). Interaction of the urea receptor with anions ( $F^-$ ,  $AcO^-$ ,  $H_2PO_4^-$ ) via hydrogen bonding or urea NH deprotonation resulted in significant fluorescence quenching of the 1,8-naphthalimide chromophore in an appropriately chosen model compound (ca. 30–45%). In the presence of both chemical input species, protons and anions, the fluorescence was also quenched. The binding of the anions by  $NH^+$  ammonium receptor has been assumed. The apparent anion binding constants of the protonated conjugate follow the basicity trend of the anions:  $AcO^- \sim F^- > H_2PO_4^-$ . The investigated system constitutes an example for the flexible and modular realization of functionally integrated INH logic at the molecular level, using protons and anions as chemical input species and the fluorescence of a PET-active signaling unit as output.

### Introduction

Processing of input information and generation of output signals, based on logic operations, is an eminent feature of information technology (IT). The implementation of logic principles at the molecular level is an interesting strategy toward nanoscale computing, based on the bottom-up approach.<sup>1–3</sup> Therefore, the realization of molecular devices with the capability of mimicking logic gates has attracted considerable interest

in recent years.<sup>4–8</sup> Nowadays, for all common Boolean logic operations used in silicon-based IT, molecular mimics are available. Many systems are based on fluorescence as optical output signal. This is not very surprising taking into account the large available pool of fluorescent compounds and their excited-state interactions via photoinduced electron transfer (PET) or energy transfer.<sup>9,10</sup>

<sup>†</sup> University of Porto.

<sup>‡</sup> Present affiliation: CQFM-IST, Technical University of Lisbon, Portugal.

<sup>§</sup> University of Huelva.

(1) Balzani, V.; Credi, A.; Venturi, M. *Chem. Eur. J.* **2002**, *8*, 5524–5532.

(2) Ball, P. *Nature* **2000**, *406*, 118–120.

(3) Collier, C. P.; Wong, E. W.; Belohradský, M.; Raymo, F. M.; Stoddart, J. F.; Kuekes, P. J.; Williams, R. S.; Heath, J. R. *Science* **1999**, *285*, 391–394.

(4) Raymo, F. M. *Adv. Mater.* **2002**, *14*, 401–414.

(5) Balzani, V.; Credi, A.; Venturi, M. *ChemPhysChem* **2003**, *4*, 49–59.

(6) de Silva, A. P.; McClenaghan, N. D. *Chem. Eur. J.* **2004**, *10*, 574–586.

(7) de Silva, A. P.; Uchiyama, S. *Nature Nanotech.* **2007**, *2*, 399–410.

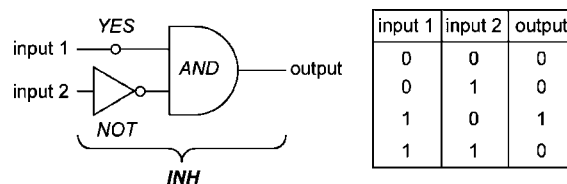
(8) Pischel, U. *Angew. Chem., Int. Ed.* **2007**, *46*, 4026–4040.

(9) de Silva, A. P.; Gunaratne, H. Q. N.; Gunnlaugsson, T.; Huxley, A. J. M.; McCoy, C. P.; Rademacher, J. T.; Rice, T. E. *Chem. Rev.* **1997**, *97*, 1515–1566.

However, very often, molecular logic operations using fluorescence outputs rely on very specific conditions dictated by structural, electronic, and spectral properties of the fluorophore, thereby limiting considerably their value in a more generalized approach. In this context, it is of high interest to develop a strategy in which the signaling fluorophore unit, and consequently the optical output, can be varied without affecting the desired logic operation. The combination of a fluorophore with PET-active receptors<sup>9</sup> linked by insulating spacers could be an interesting approach toward this goal. Such modular molecular architecture secures the general applicability to a wide range of fluorophores and therefore optical output signals, as long as PET is operative as fluorophore–receptor excited-state interaction mechanism. Thus, the logic operation is solely determined by the intelligent choice of the receptor units. Fluorophore–receptor conjugates, which behave as two- and three-input AND gates, have been reported.<sup>11–18</sup> For the latter, a combination of three receptors was used, which in individual combination with the fluorophore led to YES gates (“off–on” fluorescence switching). Conclusively, and in accordance with an AND logic operation,<sup>11</sup> the highest fluorescence signal is obtained when all receptors are occupied with the respective input species. Such systems are of high value for combinational sensing applications in solution (“lab-on-a-molecule”),<sup>18</sup> as they translate a complex analytical situation into a single optical answer signal. This example demonstrates the immediate practical value of molecular logic, especially in liquid phase, apart from eventually more speculative future applications in molecular computers.<sup>2,19</sup>

In extension of these cleverly devised AND logic gates, we decided to target the two-input inhibit (INH) gate<sup>20–28</sup> with a related strategy, based on PET-active fluorophore–receptor conjugates. INH gates are of great value for the realization of logic circuits with advanced processing capabilities, like sub-

**SCHEME 1. General Representation of an INH Gate (Formal Combination of a NOT, YES, and AND Gate) and the Corresponding Truth Table (Positive Logic; 0: Low Signal, 1: High Signal)**



tractors, comparators, or multiplexers.<sup>8,29–37</sup> Besides, as outlined for AND gates, molecular devices with INH logic behavior are also of much interest for combinational sensing, as they report on the presence of one input in simultaneous absence of another analytical parameter. As such, the two-input INH logic operation can be basically understood as an AND operation with one of the inputs being reversed. In other words, INH can be integrated<sup>38</sup> by combining a NOT, a YES, and an AND gate (Scheme 1). This points already very intuitively toward the design of a conjugate, which shows INH logic behavior. In order to ensure the specific recognition of input signals, two selective receptor units are needed. One of them should lead to fluorescence enhancement in its occupied state, equivalent to a YES operation (input 1, Scheme 1). The interaction of the other input (input 2, Scheme 1) with its corresponding receptor should lead to fluorescence quenching, thereby implementing the necessary NOT gate. The receptors (occupied or free) act in parallel on the fluorescence output signal, which implements the required AND function. In the presence of both inputs, the quenching (by input 2) should override the fluorescence enhancement by input 1, in accordance with the truth table shown in Scheme 1.

## Results and Discussion

**Molecular Approach to the Target Compound.** Our experimental design, shown in Scheme 2, uses two types of receptors that in their individual application have given rise to fluorescent chemosensors for pH and anions.<sup>9,39</sup> Receptor<sub>1</sub> is an amino function, which leads in the unprotonated state to fluorescence quenching by PET, while the corresponding ammonium ion is PET-inactive.<sup>40</sup> Thus, fluorescence enhancement upon protonation is expected. Receptor<sub>2</sub> is an urea group, known for its potential to interact with anions like AcO<sup>−</sup>, F<sup>−</sup>, or H<sub>2</sub>PO<sub>4</sub><sup>−</sup>.<sup>39,41–46</sup> It is generally accepted that the urea receptor

(10) Valeur, B. *Molecular Fluorescence: Principles and Applications*, 1st ed.; Wiley-VCH: Weinheim, 2001.

(11) de Silva, A. P.; Gunaratne, H. Q. N.; McCoy, C. P. *Nature* **1993**, *364*, 42–44.

(12) de Silva, A. P.; Gunaratne, H. Q. N.; McCoy, C. P. *J. Am. Chem. Soc.* **1997**, *119*, 7891–7892.

(13) de Silva, S. A.; Amorelli, B.; Isidor, D. C.; Loo, K. C.; Crooker, K. E.; Pena, Y. E. *Chem. Commun.* **2002**, 1360–1361.

(14) de Silva, A. P.; McClean, G. D.; Pagliari, S. *Chem. Commun.* **2003**, 2010–2011.

(15) Uchiyama, S.; McClean, G. D.; Iwai, K.; de Silva, A. P. *J. Am. Chem. Soc.* **2005**, *127*, 8920–8921.

(16) Bag, B.; Bharadwaj, P. K. *Chem. Commun.* **2005**, 513–515.

(17) Magri, D. C.; Coen, G. D.; Boyd, R. L.; de Silva, A. P. *Anal. Chim. Acta* **2006**, *568*, 156–160.

(18) Magri, D. C.; Brown, G. J.; McClean, G. D.; de Silva, A. P. *J. Am. Chem. Soc.* **2006**, *128*, 4950–4951.

(19) Credi, A. *Angew. Chem., Int. Ed.* **2007**, *46*, 5472–5475.

(20) Gunnlaugsson, T.; Mac Dónaill, D. A.; Parker, D. *Chem. Commun.* **2000**, 93–94.

(21) Gunnlaugsson, T.; Mac Dónaill, D. A.; Parker, D. *J. Am. Chem. Soc.* **2001**, *123*, 12866–12876.

(22) de Silva, A. P.; McClenaghan, N. D. *Chem. Eur. J.* **2002**, *8*, 4935–4945.

(23) de Sousa, M.; Kluciar, M.; Abad, S.; Miranda, M. A.; de Castro, B.; Pischel, U. *Photochem. Photobiol. Sci.* **2004**, *3*, 639–642.

(24) Montenegro, J.-M.; Pérez-Inestrosa, E.; Collado, D.; Vida, Y.; Suau, R. *Org. Lett.* **2004**, *6*, 2353–2355.

(25) Leigh, D. A.; Morales, M. A. F.; Pérez, E. M.; Wong, J. K. Y.; Saiz, C. G.; Slawin, A. M. Z.; Carmichael, A. J.; Haddleton, D. M.; Brouwer, A. M.; Buma, W. J.; Wurlpel, G. W. H.; León, S.; Zerbetto, F. *Angew. Chem., Int. Ed.* **2005**, *44*, 3062–3067.

(26) Banthia, S.; Samanta, A. *Eur. J. Org. Chem.* **2005**, 4967–4970.

(27) Straight, S. D.; Andréasson, J.; Kodis, G.; Bandyopadhyay, S.; Mitchell, R. H.; Moore, T. A.; Moore, A. L.; Gust, D. *J. Am. Chem. Soc.* **2005**, *127*, 9403–9409.

(28) de Sousa, M.; de Castro, B.; Abad, S.; Miranda, M. A.; Pischel, U. *Chem. Commun.* **2006**, 2051–2053.

(29) Langford, S. J.; Yann, T. *J. Am. Chem. Soc.* **2003**, *125*, 11198–11199.

(30) Margulies, D.; Melman, G.; Felder, C. E.; Arad-Yellin, R.; Shanzer, A. *J. Am. Chem. Soc.* **2004**, *126*, 15400–15401.

(31) Margulies, D.; Melman, G.; Shanzer, A. *Nat. Mater.* **2005**, *4*, 768–771.

(32) Coskun, A.; Deniz, E.; Akkaya, E. U. *Org. Lett.* **2005**, *7*, 5187–5189.

(33) Liu, Y.; Jiang, W.; Zhang, H.-Y.; Li, C.-J. *J. Phys. Chem. B* **2006**, *110*, 14231–14235.

(34) Margulies, D.; Melman, G.; Shanzer, A. *J. Am. Chem. Soc.* **2006**, *128*, 4865–4871.

(35) Pérez-Inestrosa, E.; Montenegro, J.-M.; Collado, D.; Suau, R.; Casado, J. *J. Phys. Chem. C* **2007**, *111*, 6904–6909.

(36) Andréasson, J.; Straight, S. D.; Bandyopadhyay, S.; Mitchell, R. H.; Moore, T. A.; Moore, A. L.; Gust, D. *Angew. Chem., Int. Ed.* **2007**, *46*, 958–961.

(37) Pischel, U.; Heller, B. *New J. Chem.* **2008**, *32*, 395–400.

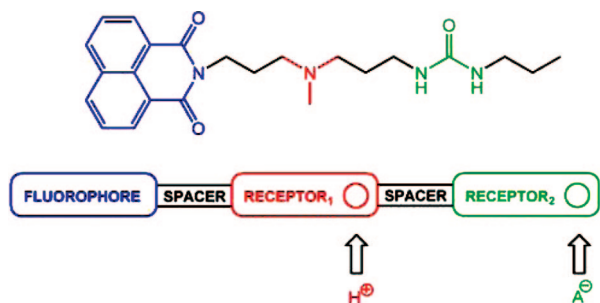
(38) de Silva, A. P.; Dixon, I. M.; Gunaratne, H. Q. N.; Gunnlaugsson, T.; Maxwell, P. R. S.; Rice, T. E. *J. Am. Chem. Soc.* **1999**, *121*, 1393–1394.

(39) Martínez-Mañez, R.; Sancenón, F. *Chem. Rev.* **2003**, *103*, 4419–4476.

(40) Daffy, L. M.; de Silva, A. P.; Gunaratne, H. Q. N.; Huber, C.; Lynch, P. L. M.; Werner, T.; Wolfbeis, O. S. *Chem. Eur. J.* **1998**, *4*, 1810–1815.

(41) Gunnlaugsson, T.; Davis, A. P.; Glynn, M. *Chem. Commun.* **2001**, 2556–2557.

**SCHEME 2. Fluorophore–Spacer–Receptor<sub>1</sub>–Spacer–Receptor<sub>2</sub> System 2 with Protons (H<sup>+</sup>) and Anions (A<sup>-</sup>) as Inputs**



becomes electron-rich upon anion recognition, which consequently leads to PET fluorescence quenching.<sup>39</sup> In our design, both receptors, the amino and the urea function, are covalently linked to a fluorophore. 1,8-Naphthalimide was chosen as fluorophore due to its well-characterized fluorescence and strong electron-accepting properties, favoring its involvement in PET-induced processes, essential for the above outlined working principle. Further, it should be emphasized that the use of insulating oligomethylene spacers leaves the inherent electronic and energetic properties of the fluorophore (redox potential, excited-state energy) independent from input recognition by the receptors. However, the spacer should be flexible enough to allow conformations with close contact between the receptor units and fluorophore, facilitating the underlying PET processes. The described molecular design of INH logic is distinct from approaches, where push–pull chromophores with excited-state ICT character were used to generate input-dependent spectral shifts by influencing the intrinsic electronic and energetic properties of the fluorophore.<sup>26,32,35</sup>

The synthesis of the target 1,8-naphthalimide derivative **2** was accomplished in two steps, outlined in Scheme 3. In the first step, excess 3,3'-diamino-*N*-methylpropylamine was condensed with 1,8-naphthalic anhydride, leading to **1** (yield 58%).<sup>47,48</sup> In a subsequent step, the free primary amino group of **1** was reacted with propyl isocyanate to afford compound **2** as a colorless solid in 79% yield.

**Fluorescence Behavior of Neutral and Protonated 2.** Compound **2** showed the typical absorption spectrum of a 1,8-naphthalimide chromophore, with a band above 300 nm (maxima at 332 and 345 nm in acetonitrile, see Supporting Information). The fluorescence spectrum ( $\lambda_{exc} = 325$  nm) corresponds to a blue emission and showed a fine-structured band with maxima at 364 and 380 nm and a shoulder at 400 nm. The fluorescence quantum yield of unprotonated **2** was estimated as  $\leq 2.4 \times 10^{-3}$ . This rather low value [compared with  $\Phi_f = 0.016$  for *N*-propyl-1,8-naphthalimide (**3**), see structure in Scheme 3b]<sup>49</sup> points to a highly efficient fluores-

cence quenching by a thermodynamically allowed PET due to the presence of the tertiary amino function in **2**. The estimation of  $\Delta G_{PET}$  with the well-known Rehm–Weller equation<sup>50</sup> ( $\Delta G_{PET} = E_{ox} - E_{red} - E^*(S_1) + C$ ) yielded strongly exergonic thermodynamics for the excited singlet state process ( $\Delta G_{PET} = -1.73$  eV, with  $E_{ox} = 0.71$  V for tri-*n*-propylamine as model,<sup>51</sup>  $E_{red} = -1.05$  V and  $E^*(S_1) = 3.43$  eV for *N*-ethyl-1,8-naphthalimide as model,<sup>52</sup>  $C = -0.06$  eV).

This situation changed completely in the presence of trifluoroacetic acid (TFA) as proton source. After addition of 1.0 equiv of TFA, the fluorescence signal was ca. 20 times higher than in absence of TFA. This observation is rationalized by the blocking of PET through protonation of the tertiary amino function. The fluorescence titration curve, observing the emission signal at 380 nm, and corresponding spectra are shown in Figure 1. The curve leveled off at 1.0 equiv as expected for formation of ammonium ion. The protonation constant could not be determined accurately as a  $\log \beta > 7$  results from the steep curvature of the titration profile (a conservative estimation led to a value of  $\log \beta = 7.9$ ).<sup>10</sup> Changes in the fluorescence intensity do not result from an alteration of intrinsic electronic properties of the naphthalimide fluorophore. This is in agreement with *ideal* PET behavior;<sup>41</sup> and as would be expected for such a situation, the absorption spectrum of **2** did not show significant variations (band shift or changes of absorbance) upon addition of protons (see Supporting Information).

**Anion Binding by the Urea Receptor.** Given the dominant fluorescence quenching of the 1,8-naphthalimide chromophore by the amino function in **2** and the resulting low fluorescence quantum yield, anion-binding properties of urea were examined more convenient for the model compound *N*-[4-(*N*-(1,8-naphthalimidyl)butyl)-*N'*-propylurea (**4**).<sup>53</sup> The urea function in **4** is embedded in the same electronic environment as in **2**, i.e., bound to the fluorophore by an insulating oligomethylene spacer. This makes the binding properties of **2** and **4** toward the investigated anions fluoride (F<sup>-</sup>), acetate (AcO<sup>-</sup>), and dihydrogenphosphate (H<sub>2</sub>PO<sub>4</sub><sup>-</sup>) directly comparable. The titration of **4** with anions (as tetra-*n*-butylammonium salts) in the millimolar concentration range led to significant fluorescence quenching (40% for 11 mM F<sup>-</sup>, 44% for 11 mM AcO<sup>-</sup>, 31% for 26 mM H<sub>2</sub>PO<sub>4</sub><sup>-</sup>), for which a PET mechanism can be assumed.<sup>39,41–44</sup> The representative example of F<sup>-</sup> is shown in Figure 2. The observed quenching is not related to an intermolecular process. This was demonstrated by the absence of a significant emission decrease (<3%) of the urea-free model compound **3** (Scheme 3b) upon addition of these anions at comparable concentrations. Further, as expected for an *ideal* PET process, no new fluorescence bands were observed, and also the characteristic absorption bands of the 1,8-naphthalimide chromophore remained virtually unaffected (see Supporting Information).

Fluorescence titrations observing the signal at 380 nm upon successive addition of anion were performed. The fitting of the

(42) Gunnlaugsson, T.; Davis, A. P.; O'Brien, J. E.; Glynn, M. *Org. Lett.* **2002**, *4*, 2449–2452.

(43) Gunnlaugsson, T.; Kruger, P. E.; Lee, T. C.; Parkesh, R.; Pfeffer, F. M.; Hussey, G. M. *Tetrahedron Lett.* **2003**, *44*, 6575–6578.

(44) Gunnlaugsson, T.; Davis, A. P.; Hussey, G. M.; Tierney, J.; Glynn, M. *Org. Biomol. Chem.* **2004**, *2*, 1856–1863.

(45) Esteban-Gómez, D.; Fabbri, L.; Licchelli, M.; Monzani, E. *Org. Biomol. Chem.* **2005**, *3*, 1495–1500.

(46) Gunnlaugsson, T.; Glynn, M.; Tocci, G. M.; Kruger, P. E.; Pfeffer, F. M. *Coord. Chem. Rev.* **2006**, *250*, 3094–3117.

(47) Braña, M. F.; Castellano, J. M.; Morán, M.; Pérez de Vega, M. J.; Qian, X. D.; Romerdahl, C. A.; Keilhauer, G. *Eur. J. Med. Chem.* **1995**, *30*, 235–239.

(48) Licchelli, M.; Orbelli Biroli, A.; Poggi, A.; Sacchi, D.; Sangermani, C.; Zema, M. *J. Chem. Soc., Dalton Trans.* **2003**, 4537–4545.

(49) Jones, G., II; Kumar, S. *J. Photochem. Photobiol. A: Chem.* **2003**, *160*, 139–149.

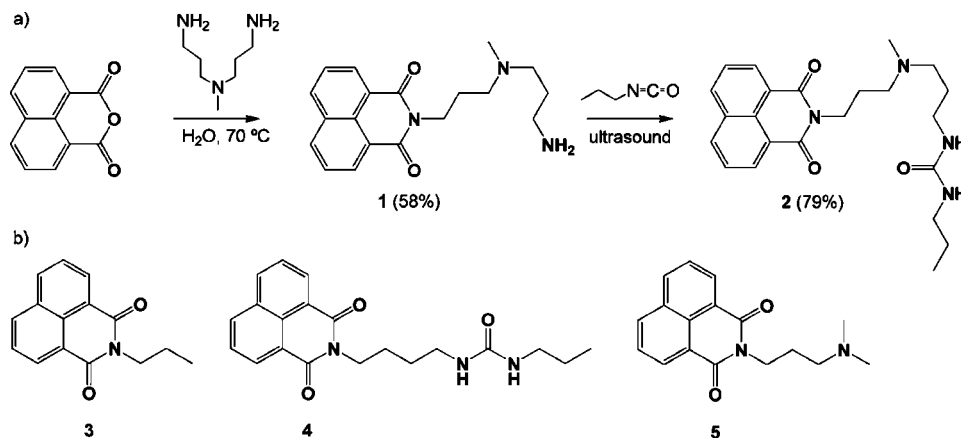
(50) Rehm, D.; Weller, A. *Ber. Bunsenges. Phys. Chem.* **1969**, *73*, 834–839.

(51) Pischel, U.; Nau, W. M. *J. Phys. Org. Chem.* **2000**, *13*, 640–647.

(52) Ramachandram, B.; Saroja, G.; Sankaran, N. B.; Samanta, A. *J. Phys. Chem. B* **2000**, *104*, 11824–11832.

(53) Upon addition of small amounts of anions to **2** in acetonitrile, some fluorescence quenching was observed, which is most likely the result of their interaction with the amine-corresponding ammonium ion (see discussion of anion interaction with protonated **2** and **5**). Given the high basicity of the aliphatic amine unit, traces protons from the acetonitrile solvent are already sufficient to form small amounts of ammonium.

**SCHEME 3. (a) Synthesis of Fluorophore–Spacer–Receptor<sub>1</sub>–Spacer–Receptor<sub>2</sub> Conjugate 2. (b) Structures of Model Compounds 3–5**



obtained titration curves yielded typical binding constants involving aliphatic urea units, which are of comparable order of magnitude as reported for related (thio)urea receptors.<sup>44,54–57</sup> Namely,  $\log \beta_{11}$  values of  $2.33 \pm 0.1$ ,  $2.35 \pm 0.1$ , and  $1.89 \pm 0.1$  were obtained for  $F^-$ ,  $AcO^-$ , and  $H_2PO_4^-$ , respectively. For urea receptors with aromatic electron-withdrawing substituents, it has been shown that NH deprotonation can occur.<sup>58–61</sup> The NH acidity of alkyl-substituted urea, as in compound **2** or **4**, should be not sufficiently high to yield deprotonation by  $AcO^-$  or  $H_2PO_4^-$ . However, in the case of  $F^-$ , the possible formation of  $HF_2^-$  constitutes a considerable driving force for at least partial deprotonation of the urea NH.<sup>45</sup>

In order to gain further insight in the complexation of the anions by the urea unit, <sup>1</sup>H NMR measurements in dimethyl-

sulfoxide-*d*<sub>6</sub> were performed. Solutions of **2** were titrated with  $F^-$ ,  $AcO^-$ , or  $H_2PO_4^-$  anions, and the shift of the urea NH protons was monitored (Figure 3). In the absence of anions, a single signal for the urea NH protons was observed at 5.75 ppm. Upon addition of anions, this signal broadened and experienced a gradual low-field shift. These observations are in agreement with related reports about interactions of these anions with urea and thiourea receptors.<sup>44,62</sup> Pronounced chemical shift changes were observed for  $F^-$  ( $\Delta\delta = 1.50$  ppm for 5 equiv of anion) and  $AcO^-$  ( $\Delta\delta = 1.39$  ppm for 12 equiv of anion). For  $H_2PO_4^-$  the changes were less dramatic, but still significant ( $\Delta\delta = 0.74$  ppm for 18 equiv of anion). The obtained titration curves are shown in Figure 4. The application of a 1:1 binding model led to satisfying fits and binding constants  $\log \beta_{11}$  of  $1.63 \pm 0.1$ ,  $1.30 \pm 0.1$ , and  $1.23 \pm 0.2$  for  $F^-$ ,  $AcO^-$ , and  $H_2PO_4^-$ , respectively. In comparison to fluorescence titrations, slightly lower absolute values of anion binding obtained from the <sup>1</sup>H NMR experiments might be qualitatively accounted for self-aggregation phenomena (e.g., urea–urea hydrogen bonding) of ligand **2** (8–10 mM) and competition with the hydrogen-bond accepting solvent dimethyl sulfoxide-*d*<sub>6</sub>.

**Fluorescence Behavior of Protonated 2 in Presence of Anions.** So far, the fluorescence behavior of the 1,8-naphthalimide chromophore in the absence of any chemical input information or the presence of protons or anions was discussed. In the presence of 1.0 equiv of protons, the fluorescence of **2** is switched on; however, the addition of anions (1.0 equiv of  $AcO^-$ , 1.5 equiv of  $F^-$ , 2.9 equiv of  $H_2PO_4^-$ ) to monoprotonated **2** led to complete fluorescence quenching. In Figure 5, the example of the titration with  $F^-$  ions is shown. On the basis of studies concerning anion binding to the urea receptor in model

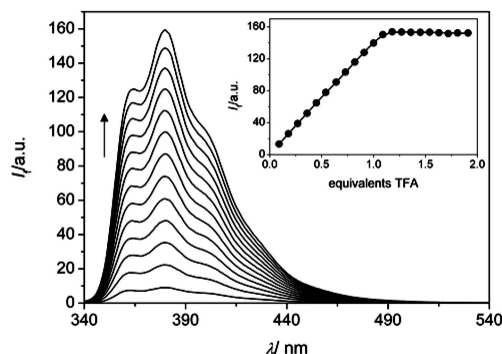


**FIGURE 1.** Fluorescence spectra of **2** (11.4  $\mu$ M) in acetonitrile upon addition of TFA. The inset shows the fluorescence titration curve at  $\lambda_{\text{obs}} = 380$  nm.

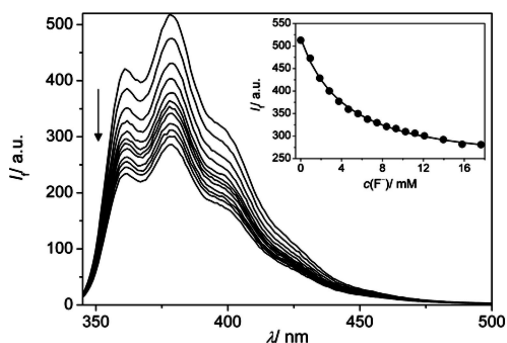


**FIGURE 2.** Fluorescence spectra of **4** (10  $\mu$ M) in acetonitrile upon addition of  $Bu_4NF$ . The inset shows the fluorescence titration curve at  $\lambda_{\text{obs}} = 380$  nm.

(54) Fan, E.; van Arman, S. A.; Kincaid, S.; Hamilton, A. D. *J. Am. Chem. Soc.* **1993**, *115*, 369–370.

(55) Nishizawa, S.; Bühlmann, P.; Iwao, M.; Umezawa, Y. *Tetrahedron Lett.* **1995**, *36*, 6483–6486.

(56) Linton, B. R.; Goodman, M. S.; Fan, E.; van Arman, S. A.; Hamilton, A. D. *J. Org. Chem.* **2001**, *66*, 7313–7319.

(57) Gunnlaugsson, T.; Davis, A. P.; O'Brien, J. E.; Glynn, M. *Org. Biomol. Chem.* **2005**, *3*, 48–56.

(58) Boiocchi, M.; Del Boca, L.; Esteban-Gómez, D.; Fabbrizzi, L.; Licchelli, M.; Monzani, E. *J. Am. Chem. Soc.* **2004**, *126*, 16507–16514.

(59) Boiocchi, M.; Del Boca, L.; Esteban-Gómez, D.; Fabbrizzi, L.; Licchelli, M.; Monzani, E. *Chem. Eur. J.* **2005**, *11*, 3097–3104.

(60) Esteban-Gómez, D.; Fabbrizzi, L.; Licchelli, M. *J. Org. Chem.* **2005**, *70*, 5717–5720.

(61) Amendola, V.; Esteban-Gómez, D.; Fabbrizzi, L.; Licchelli, M. *Acc. Chem. Res.* **2006**, *39*, 343–353.

(62) Kim, S. K.; Singh, N. J.; Kim, S. J.; Swamy, K. M. K.; Kim, S. H.; Lee, K.-H.; Kim, K. S.; Yoon, J. *Tetrahedron* **2005**, *61*, 4545–4550.

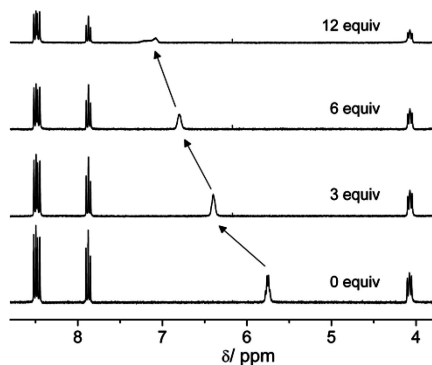


**FIGURE 3.** Partial  $^1\text{H}$  NMR spectra of **2** (7.9 mM) in dimethyl sulfoxide- $d_6$  in the absence and presence of  $\text{Bu}_4\text{NAcO}$  (3, 6, and 12 equiv).

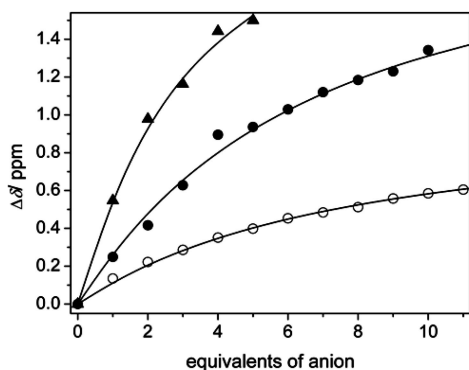


**FIGURE 4.** Chemical shift changes ( $\Delta\delta$ ) of urea NH protons of **2** (7.9–9.8 mM) in dimethyl sulfoxide- $d_6$  upon addition of  $\text{F}^-$  (filled triangles),  $\text{AcO}^-$  (filled circles), and  $\text{H}_2\text{PO}_4^-$  (empty circles).

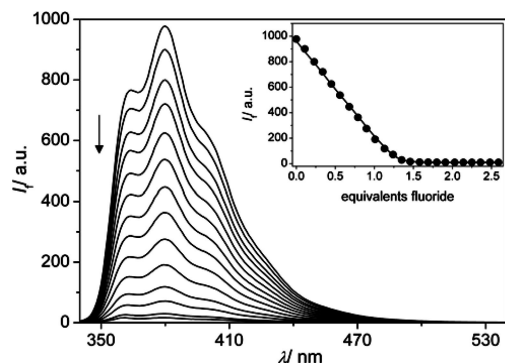


**FIGURE 5.** Fluorescence spectra of monoprotonated **2** (11.4  $\mu\text{M}$ ) in acetonitrile upon addition of  $\text{Bu}_4\text{NF}$ . The inset shows the fluorescence titration curve at  $\lambda_{\text{obs}} = 380$  nm.

compound **4**, such low concentrations (micromolar range) are not sufficient to explain the quenching via PET from an anion–urea complex. In order to rationalize the observations, control experiments with monoprotonated  $N$ -(3-( $N,N'$ -dimethylamino)propyl)-1,8-naphthalimide (**5**, see structure in Scheme 3b), which lacks a urea receptor, were performed. This led as well to anion-induced fluorescence quenching (>95%). In these cases, the titration curves leveled off at ca. 1.0 equiv of  $\text{AcO}^-$  and  $\text{F}^-$  and 2.5 equiv of  $\text{H}_2\text{PO}_4^-$ . The observations with monoprotonated **5** corroborate that the ammonium ion in monoprotonated **2** is actively involved, not only in the binding of the anions<sup>63</sup> but also in the fluorescence quenching through

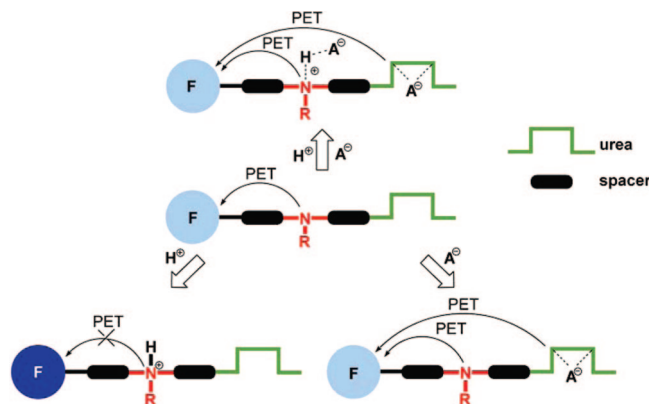
(63) Huston, M. E.; Akkaya, E. U.; Czarnik, A. W. *J. Am. Chem. Soc.* **1989**, *111*, 8735–8737.

**TABLE 1.** Binding Constants of Various Anions with Monoprotonated **2** and **5**

anion	ligand/anion ( $i:j$ )	$\log \beta_{ij}$	
		$2\text{H}^{+a}$	$5\text{H}^{+a}$
$\text{AcO}^-$	1:1	$>7^b$	$>7^b$
$\text{F}^-$	1:1	$>7^b$	$>7^b$
$\text{H}_2\text{PO}_4^-$	1:1	5.8	5.8
	1:2	12.0	12.0
	2:1	12.9	12.1

<sup>a</sup>  $2\text{H}^+$ : monoprotonated **2**.  $5\text{H}^+$ : monoprotonated **5**. <sup>b</sup> Accurate determination of binding constants was prevented by the steep curvature of the titration plots.

**SCHEME 4.** Summarized PET Behavior of Conjugate **2** with Proton ( $\text{H}^+$ ) and Anion ( $\text{A}^-$ ) Inputs<sup>a</sup>



<sup>a</sup> The fluorescence output is color-coded (dark blue: strongly fluorescent, light-blue: weakly fluorescent).

the formed complex. It can be assumed that the binding of anions by the ammonium ion via hydrogen bonding and electrostatic interactions<sup>39</sup> leads to a weakening of the  $\text{NH}^+$  bond and reactivation of the PET-induced fluorescence quenching.

The fluorescence titration curves of monoprotonated **2** and **5** were fitted according to appropriate binding models, and the obtained association constants are summarized in Table 1. The best fitting resulted from the application of a 1:1 binding model in the cases of  $\text{AcO}^-$  and  $\text{F}^-$ , while for  $\text{H}_2\text{PO}_4^-$  a 1:2 complex with two anions per molecule of monoprotonated ligand and a 2:1 complex with two ligands per anion had to be invoked.<sup>64</sup> A comparison of the 1:1 binding constants for monoprotonated **5** revealed the order of  $\text{AcO}^- \sim \text{F}^- > \text{H}_2\text{PO}_4^-$ , which parallels the basicities of the anions. The same trend was observed for  $\log \beta_{11}$  values with monoprotonated **2**.

**Logic Behavior of 2 with Protons and Anions as Inputs.** The PET behavior, and consequently the fluorescence (output) properties, of **2** in the presence and absence of chemical input information (Scheme 4) can be interpreted within the framework of molecular logic. The absence of input (protons, anions) or output values (fluorescence intensity) below a predefined threshold level are translated into binary “0”, while the presence of an input or fluorescence outputs above the threshold correspond to binary “1”, in accordance with positive logic convention. The strong fluorescence enhancement with protons and the low fluorescence signal in presence of anions led to the definition of a very low output threshold level of 10%

(64) The involvement of a 2:1 species is supported by the appearance of a significant broad shoulder at ca. 470 nm in the emission spectrum upon addition of  $\text{H}_2\text{PO}_4^-$  (see the Supporting Information), which could be assigned to an excimer emission as observed earlier for 1,8-naphthalimide derivatives (ref. 49).

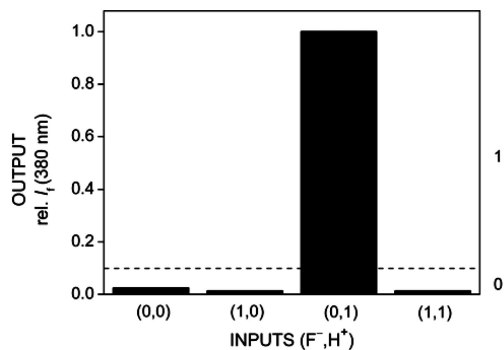


**FIGURE 6.** Summary of the fluorescence response of **2** (10  $\mu\text{M}$ ) with different input combinations of  $\text{F}^-$  ions (11 mM) and protons (10  $\mu\text{M}$ ). The threshold level is marked with a dashed line.

of the highest fluorescence signal. Thus, practically an all (“1”) or nothing (“0”) situation is created. This is very important with respect to clear and unambiguous logic decisions. In our approach, the threshold level is determined by the fluorescence enhancement upon protonation of the electron-donating amino function. The more efficient the quenching by PET from the amine, the higher the fluorescence enhancement factor. This in turn can be implemented by exergonic PET thermodynamics (strong electron-accepting fluorophores) and the use of flexible spacers, enabling short effective distances between electron donor and acceptor.

In agreement with the general formulation of an INH gate (cf. Scheme 1), the strongest fluorescence signal (output: “1”) of the 1,8-naphthalimide unit is observed in the presence of protons (input 1: “1”) and absence of anions (input 2: “0”). For all other input combinations, an output signal below the threshold level was obtained (output: “0”). The formation of ammonium in presence of protons creates an additional binding mode for anions via hydrogen bonding and electrostatic interactions. Thus, for the simultaneous presence of both inputs their parallel recognition by the molecular logic gate applies. Noteworthy, although the quenching by the amino function in **2** is certainly more efficient than the PET quenching by the urea–anion complex, it is important to mention that the urea receptor behaves like a NOT gate as conceptually required by an INH function. Scheme 4 summarizes the global picture, based on enabling or blocking of PET processes, which corresponds to low or high fluorescence signals, respectively. In Figure 6 detailed fluorescence outputs in dependence on the four possible binary input combinations are given for the representative example of  $\text{F}^-$  ions and protons as inputs. The other two anions ( $\text{AcO}^-$  and  $\text{H}_2\text{PO}_4^-$ ) gave rise to a very similar picture.

As outlined above, the combination of a YES (amine) and a NOT receptor (urea) linked to a PET-active fluorophore leads indeed to molecular INH logic. Importantly, the modular molecular design based on a PET conjugate will enable flexible fine-tuning of the fluorescence output signal of the chosen photoactive unit. In general, this should be always applicable for electron-accepting fluorophores, leading to favorable PET thermodynamics. Thus, also ICT fluorophores like the closely related 4-amino-1,8-naphthalimide could be integrated. However, as studies with model compounds have shown,<sup>65</sup> additional criteria like molecular electric field effects on PET should be taken into account in the design of conjugates containing ICT fluorophores.

## Conclusions

The fluorophore–spacer–receptor<sub>1</sub>–spacer–receptor<sub>2</sub> conjugate **2** was used for the modular functional integration of two-input INH molecular logic. The conjugate, containing 1,8-naphthalimide as electron-accepting photoactive unit and amino and urea receptors for protons and anions, respectively, shows *ideal* PET behavior. Protonation of the amino group leads to drastic fluorescence enhancement, due to the blocking of PET. On the other hand, anions bind to the urea receptor, as demonstrated by the resulting fluorescence quenching by PET (conveniently shown with model compound **4**) and chemical shift changes for the urea NH protons, observed in <sup>1</sup>H NMR titrations. Simultaneous presence of protons and anions as input information, yields also fluorescence quenching. Supposedly, in the latter case, anion binding to the  $\text{NH}^+$  ammonium is involved. The global fluorescence behavior of **2** is in accordance with the logic INH function, which is straightforward integrated by the combination of receptor units that separately behave like YES and NOT logic gates and influence in parallel (AND gate) the fluorescence of the photoactive signaling unit.

The modular architecture composed of fluorophore, YES and NOT receptor, and insulating spacers is expected to be adaptable to a variety of photoactive signaling units, as long as the underlying PET processes are thermodynamically favored. This opens interesting perspectives for the tailored implementation of INH logic with a wide range of spectral output signals.

## Experimental Section

**Materials.** All starting materials for the synthesis are commercially available and have been used as received (purity >98%). Acetonitrile was of HPLC quality. All other reagents (tetra-*n*-butylammonium salts of the anions and trifluoroacetic acid) were of highest purity (>99%) available and used without further purification. Solvents for NMR measurements had a deuteration grade of >99 atom D%. Compounds **1**,<sup>47</sup> **3**,<sup>49</sup> and **5**<sup>52</sup> have been reported in the literature.

**Spectroscopic Measurements.** Absorption and fluorescence measurements were done in acetonitrile with standard instrumentation. NMR measurements were performed with a 300 MHz spectrometer. The fluorescence quantum yield of **2** was measured with *N*-propyl-1,8-naphthalimide as standard ( $\Phi_f = 0.016$  in acetonitrile under air).<sup>49</sup> Fluorescence titrations ( $\lambda_{\text{exc}} = 325$  nm) were performed by stepwise addition of a stock solution of trifluoroacetic acid or the respective tetra-*n*-butylammonium salt to a cuvette (1 cm optical path length) containing the fluorophore conjugate (10.0–11.4  $\mu\text{M}$ ) in its neutral or protonated form. Special care was taken to minimize dilution effects during the titration (maximum of 200  $\mu\text{L}$  stock solution to 4 mL solution in cuvette) and to allow the solution to equilibrate after each addition (ca. 10–15 min). Titration curves were fitted with HYPERQUAD 2003<sup>66,67</sup> (fluorescence) or NMRTit (NMR).<sup>68</sup>

**Preparation of Compound 2:** *N*-[3-([3-(*N*-(1,8-Naphthalimidyl)propyl)methylamino)propyl]-*N'*-propylurea. To 85 mg (0.26 mmol) of *N*-[3-[(3-aminopropyl)methylamino]propyl]-1,8-naphthalimide (**1**) was added 2.5 mL of propyl isocyanate (26.7 mmol). The suspension was treated in an ultrasonic bath for 5 min, during which time a white precipitate formed. Subsequently, 5 mL

(65) de Silva, A. P.; Gunaratne, H. Q. N.; Habib-Jiwan, J.-L.; McCoy, C. P.; Rice, T. E.; Soumilion, J.-P. *Angew. Chem., Int. Ed. Engl.* **1995**, *34*, 1728–1731.

(66) Gans, P.; Sabatini, A.; Vacca, A. *Talanta* **1996**, *43*, 1739–1753.

(67) Alderighi, L.; Gans, P.; Ienco, A.; Peters, D.; Sabatini, A.; Vacca, A. *Coord. Chem. Rev.* **1999**, *184*, 311–318.

(68) Iwanaga, T.; Nakamoto, R.; Yasutake, M.; Takemura, H.; Sako, K.; Shinmyozu, T. *Angew. Chem., Int. Ed.* **2006**, *45*, 3643–3647.

of acetonitrile was added, and the solid was filtered off and washed with small amounts of acetonitrile. After vacuum drying, 85 mg (79% yield) of a colorless solid was obtained. Samples used in photophysical measurements were subjected prior to column chromatography (aluminum oxide, chloroform/ethylacetate 10/1) and/or recrystallization from acetonitrile:  $^1\text{H}$  NMR ( $\text{CDCl}_3$ , 300 MHz)  $\delta$  8.58 (d,  $J = 7.3$  Hz, 2H), 8.25 (d,  $J = 7.4$  Hz, 2H), 7.78 (m, 2H), 6.00 (br s, 1H), 5.33 (br s, 1H), 4.29–4.24 (m, 2H), 3.38–3.32 (br m, 2H), 3.22–3.15 (m, 2H), 2.48–2.44 (m, 4H), 2.21 (s, 3H), 1.94–1.85 (m, 2H), 1.59–1.47 (m, 2H), 0.91 (t,  $J = 7.4$  Hz, 3H). *Note:* In chloroform-*d*, the signal of two protons was hidden under a broad water signal between 1.73 and 1.63 ppm. Therefore, the measurement of the  $^1\text{H}$  NMR spectrum was repeated in acetonitrile-*d*<sub>3</sub>:  $^1\text{H}$  NMR ( $\text{CD}_3\text{CN}$ , 300 MHz)  $\delta$  8.54 (d,  $J = 7.3$  Hz, 2H), 8.35 (d,  $J = 8.3$  Hz, 2H), 7.82 (dd,  $J = 7.3, 8.3$  Hz, 2H), 5.39 (br s, 1H), 5.09 (br s, 1H), 4.19–4.14 (m, 2H), 3.17–3.11 (m, 2H), 3.05–2.99 (m, 2H), 2.43 (t,  $J = 6.7$  Hz, 2H), 2.36 (t,  $J = 6.6$  Hz, 2H), 2.18 (s, 3H), 1.90–1.80 (m, 2H), 1.61–1.53 (m, 2H), 1.48–1.36 (m, 2H), 0.85 (t,  $J = 7.4$  Hz, 3H);  $^{13}\text{C}$  NMR ( $\text{CDCl}_3$ , 75 MHz)  $\delta$  164.5, 159.2, 134.4, 131.8, 131.4, 128.4, 127.1, 122.6, 56.0, 55.3, 42.3, 42.1, 39.2, 39.1, 26.8, 25.7, 23.8, 11.6. Anal. Calcd

for  $\text{C}_{23}\text{H}_{30}\text{N}_4\text{O}_3$ : C, 67.29; H, 7.37; N, 13.65. Found: C, 66.93; H, 7.60; N, 13.66.

Model compound **4** has been prepared in a very similar way. Experimental details and spectroscopic information can be found in the Supporting Information.

**Acknowledgment.** The financial support by the Spanish Ministry of Science and Education, Madrid (Ramón y Cajal grant to U.P.), and the Portuguese Foundation for Science and Technology (FCT), Lisbon (PhD fellowship SFRH/BD/18699/2004 for M.K.; postdoctoral fellowship SFRH/BPD/34384/2006 for R.F.; research grant POCI/QUI/58535/2004), is gratefully acknowledged. We thank Prof. A. P. de Silva (Queen's University Belfast) for helpful discussions.

**Supporting Information Available:** Synthetic procedures for **1** and **4**, NMR data of **1–5**, and UV/vis absorption spectra of **2** and **4**, upon addition of protons or anions, respectively. This material is available free of charge via the Internet at <http://pubs.acs.org>.

JO800342T